

# Effect of carbon coating on the superconducting properties of Pb and Sn nano-spheres

L. Shani <sup>1</sup>, V. B. Kumar <sup>2</sup>, A. Gedanken <sup>2</sup>, A. Shaulov <sup>1</sup>, and Y. Yeshurun <sup>1</sup>

<sup>1</sup>Department of Physics and Institute of Nanotechnology and Advanced Materials, Bar-Ilan University, 52900 Ramat-Gan, Israel

<sup>2</sup>Department of Chemistry and Institute of Nanotechnology and Advanced Materials, Bar-Ilan University, 52900 Ramat-Gan, Israel

**Abstract.** Carbon coated Sn and Pb spheres of radius smaller than the superconducting coherence length of the bulk materials were fabricated using a sonochemical technique. Both samples reveal Type-I superconducting behavior characterized by supercritical fields. Analysis of the data reveal the expected enhancement of the critical field,  $H_c$ , in the Pb but not in the Sn nano-spheres. The different behavior of the Sn spheres is attributed to carbon doping which results in a decrease of their effective coherence length to below the spheres size.

## Introduction

Superconductors of size smaller than the coherence length exhibit significant different properties than the bulk materials [1, 2]. A notable example is the dramatically enhanced critical field,  $H_c$ , in nano-size Type-I superconductors [3-5]. A pitfall in characterizing nano-particles may arise from agglomeration and/or oxidation of the nano-particles. This is commonly prevented by coating the particles with various materials. In this paper we describe magnetic measurements in carbon coated Pb and Sn nano-spheres, indicating that the coating process may cause doping of the material, thus reducing the effective coherence length to below the particles size leading to elimination of size effects. Such a phenomenon occurs in Sn but absent in Pb for a reason to be explained below.

## Experimental

Granules of pure Sn and Pb metals were melted in silicone oil in a separate quartz test tubes. The mixture was irradiated for 5 minutes with 20 kHz ultrasonic energy, forming a suspension of particles in the Si-oil. After precipitation, the particles were separated using a centrifuge, washed several times with n-hexane and dried in vacuum. X-ray diffraction of both elements showed the existence of only Pb and Sn confirming the purity of the samples. The size distribution of the nano-particles was measured using Dynamic Light Scattering (DLS). These measurements showed an average particle size of ~120 and ~70 nm with a full width at half maximum of ~20 nm for Sn and Pb, respectively. The magnetic measurements described in the next section were performed using a Superconducting Quantum Interference Device (SQUID - Quantum Design MPMS-5XL) magnetometer.

## Results and Discussion

Figure 1 shows magnetization curves for the Pb (upper panel) and Sn samples measured at the indicated temperatures, for increasing and decreasing fields. Both samples exhibit characteristics of type-I superconductors, namely magnetic hysteresis with superheating,  $H_{sh}$ , and supercooling,  $H_{sc}$ , fields (marked by arrows for the lowest temperature of each sample) [6]. The temperature dependence of  $H_{sh}$  and  $H_{sc}$  for both samples is shown in Figure 2. From these data one can deduce  $H_c$  and the Ginzburg-Landau parameter  $\kappa$ , based on the equations derived by Feder *et al.* for spherical type-I superconductors [7]:

$$H_{sh} = \frac{2}{3} 2^{-1/4} \kappa^{-1/2} H_c \quad (1)$$

$$H_{sc} = 1.69 \sqrt{2} \kappa H_c. \quad (2)$$

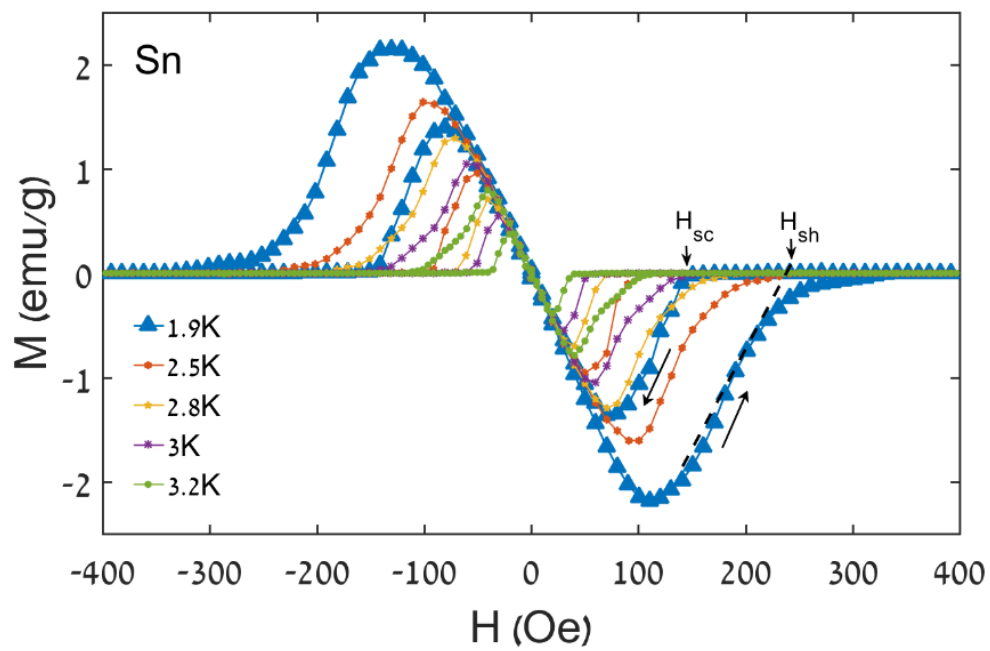
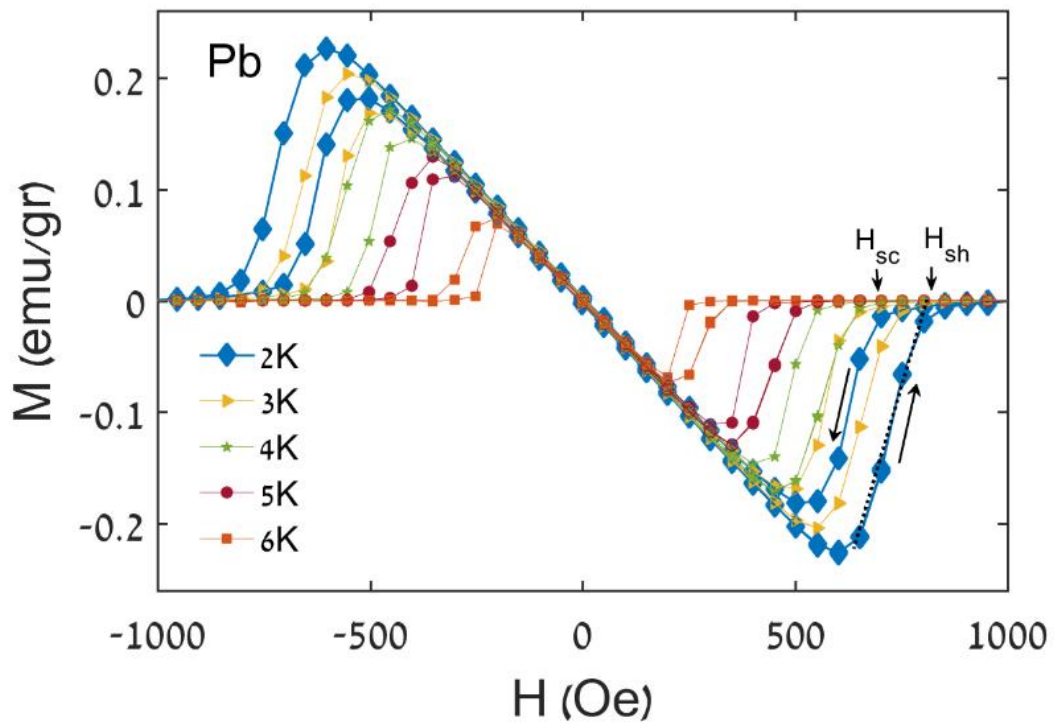


**Figure 1.** Magnetization curves at different temperatures for Pb (upper panel) and Sn nano-spheres. Arrows indicate increasing and decreasing fields for the lowest temperatures.

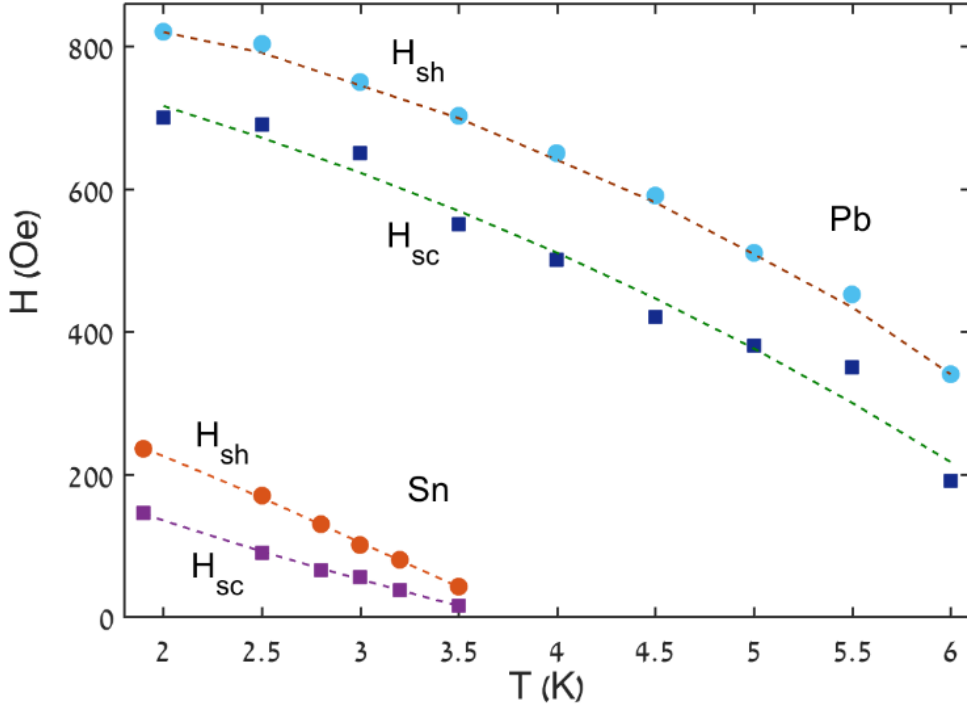


**Figure 2.** Temperature dependence of the superheating fields (circles) and the supercooling fields (squares) for the Pb and Sn samples. Dashed lines are guide to the eye.

These two equations yield:

$$H_c = 1.1(H_{sc}H_{sh}^2)^{1/3}, \quad (3)$$

and

$$\kappa = 0.38(H_{sc}/H_{sh})^{2/3}. \quad (4)$$

Figure 3 shows the values of  $H_c$  for both samples as a function of temperature, derived from Eq. (3). The solid lines are fits to the empirical approximation  $H_c = H_c(0)(1 - (T/T_c)^2)$ , yielding the values 305 and 950 Oe for  $H_c(0)$  in the Sn and Pb nano-spheres, respectively. We note that while the  $H_c(0)$  value for the Sn nano-spheres are close to that for bulk (300 Oe),  $H_c(0)$  for the Pb nano-spheres is significantly higher than the bulk value (800 Oe) [8]. The increase of  $H_c(0)$  for the Pb nano-spheres is consistent with previous reports of enhanced critical field in type-I nano-particles (see, e.g. [8, 9]). The result for Sn, however, is inconsistent with these reports (see, e.g.[3]).

We argue that the size effect in Sn is eliminated by a significant reduction of the coherence length to a value smaller than the size of the sample, due to carbon doping of the spheres. This is indicated by a significant increase in  $\kappa(0)$  relative to a clean Sn bulk, estimated as follows. We approximate the value of  $\kappa(T_c)$  by inserting in Eq. (4) the values of  $H_{sh}$  and  $H_{sc}$  at the highest measured temperature (3.2 K in Sn), yielding  $\kappa(T_c) \approx 0.18$ . Using the empirical approximation  $\kappa(T) = \kappa(0)/(1 + (T/T_c)^2)$  [6] yields  $\kappa(0) \approx 0.36$ , which is significantly higher than the reported value of 0.15 for clean bulk Sn [8]. To estimate the value of the effective coherence length,  $\xi_{eff}$ , for this sample we use the equation [10]:

$$\xi_{eff} = \xi_0 l / (\xi_0 + l). \quad (5)$$

where the value of the electron mean free path,  $l$ , is estimated using the dirty limit formula [6]

$$\kappa(T_c) = \frac{0.72\lambda_L(0)}{l}. \quad (6)$$

Insertion of the values  $\kappa(T_c) \approx 0.18$  and  $\lambda_L(0) = 34 \text{ nm}$  in Eq. (6), yields  $l = 129 \text{ nm}$ . With  $\xi_0 \approx 230 \text{ nm}$ , Eq. (5) yields  $\xi_{\text{eff}} = 83 \text{ nm}$ . This value of  $\xi_{\text{eff}}$  is smaller than the size of the sample ( $\sim 120 \text{ nm}$ ), thus no size-effect is expected for the Sn spheres.

Similar calculation for the Pb sample yields  $\kappa(T_c) \approx 0.23$ , implying  $\kappa(0) \approx 0.46$ , which is close to that of a clean bulk sample (0.44 in [8]). This result suggest that the Pb nano-spheres are unaffected by the carbon coating and, therefore, exhibit the expected size effect in  $H_c$  described above. The fact that the Pb spheres are 'clean' whereas the Sn spheres are 'dirty', although they went through the same carbon coating process, is explained by the fact that Pb, unlike Sn, does not dissolve carbon and does not interact with it to form chemical bonds[11].

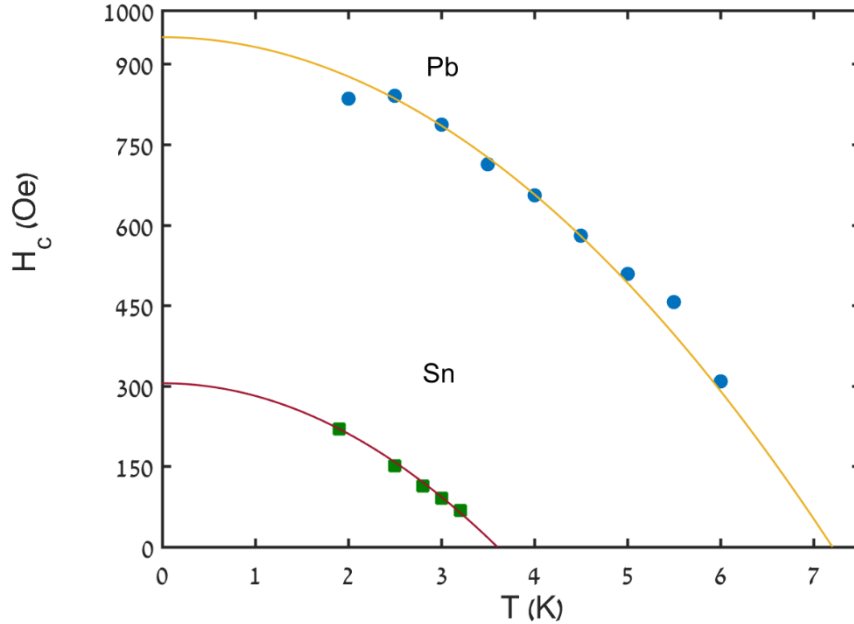


**Figure 3.** Calculated temperature dependence of the critical field,  $H_c$ , for samples Pb and Sn, as deduced from Eq. (3), see text. The solid lines through the data points are fits to the empirical approximation  $H_c = H_{c0}(1 - (T/T_c)^2)$  with  $H_{c0} = 950$  and 305 Oe for Pb and Sn, respectively.

### Summary and Conclusions

Magnetic measurements in carbon-coated Sn and Pb nano-spheres, with size smaller than the coherence length,  $\xi_0$ , of the clean material, show a significant increase of  $H_c$  in the Pb but not in the Sn spheres. The absence of an increase in  $H_c$  in the Sn spheres is attributed to carbon doping of the Sn during the coating process. The doping results in a decrease in the effective coherence length to below the spheres size, thus eliminating the size effect. Doping of the Pb nano-spheres by carbon is less effective because Pb does not dissolve carbon and does not interact with it to form chemical bonds.

**Acknowledgements.** This work was partially supported by the Israel Science Foundation (ISF) and the German-Israeli Foundation (GIF).

## References

- [1] Prozorov R 2007 Equilibrium topology of the intermediate state in type-I superconductors of different shapes *Physical Review Letters* **98** 257001
- [2] Li W-H, Wang C-W, Li C-Y, Hsu C, Yang C and Wu C-M 2008 Coexistence of ferromagnetism and superconductivity in Sn nanoparticles *Physical Review B* **77** 094508
- [3] Giaever I and Zeller H 1968 Superconductivity of small tin particles measured by tunneling *Physical Review Letters* **20** 1504
- [4] Zhang Y, Wong C H, Shen J, Sze S T, Zhang B, Zhang H, Dong Y, Xu H, Yan Z and Li Y 2016 Dramatic enhancement of superconductivity in single-crystalline nanowire arrays of Sn *Scientific Reports* **6**
- [5] Wang X-L, Feygenson M, Aronson M C and Han W-Q 2010 Sn/SnO<sub>x</sub> Core– Shell Nanospheres: Synthesis, Anode Performance in Li Ion Batteries, and Superconductivity *The Journal of Physical Chemistry C* **114** 14697-703
- [6] Tinkham M 2004 *Introduction to Superconductivity*: Dover Books on Physics
- [7] Feder J and McLachlan D S 1969 Superheating and supercooling in single spheres of tin, indium, and gold-plated indium *Physical Review* **177** 763
- [8] Bose S and Ayyub P 2014 A review of finite size effects in quasi-zero dimensional superconductors *Reports on Progress in Physics* **77** 116503
- [9] Reich S, Leitus G, Popovitz-Biro R and Schechter M 2003 Magnetization of small lead particles *Physical Review Letters* **91** 147001
- [10] Huebener R 2001 *Magnetic flux structures in superconductors: extended reprint of a classic text*: Springer Science & Business Media
- [11] Banhart F, Hernandez E and Terrones M 2003 Extreme superheating and supercooling of encapsulated metals in fullerenelike shells *Physical review letters* **90** 185502